ELSEVIER

Journal of Fluids and Structures 23 (2007) 1077–1092

JOURNAL OF FLUIDS AND STRUCTURES

www.elsevier.com/locate/jfs

On modelling and linear vibrations of arbitrarily sagged inclined cables in a quiescent viscous fluid

S.V. Sorokin[a,*], G. Rega[b]

[a]*Institute of Mechanical Engineering, Aalborg University, Pontoppidanstraede 101, DK 9220 Aalborg, Denmark*
[b]*Dipartimento di Ingegneria Strutturale e Geotecnica, Universita' di Roma La Sapienza, Via A. Gramsci 53, 00197 Roma, Italy*

Received 27 February 2006; accepted 6 April 2007
Available online 15 June 2007

Abstract

A theory of free linear vibrations of arbitrarily sagged inclined cables in a viscous fluid is presented in the framework of the heavy fluid loading concept. The static equilibrium shape of the cable is found by using the model of inextensible catenary and the validity ranges of this approximation are assessed. The dynamics of the viscous fluid is described by the linearised Navier–Stokes equations and their solution is pursued analytically by formulating the fluid field variables via potential functions. The vibration problem of a submerged cable is solved by Galerkin's method and the modal added mass and modal viscous damping coefficients are calculated. As a prerequisite for this analysis, the free vibrations of a cable in vacuum are addressed and a very good agreement with known results is observed. The physical interpretation of the dependence of modal added mass and modal damping coefficients on the 'design variables' for a fluid-loaded cable is given and the possible extensions of the suggested theory to capture weakly nonlinear effects are highlighted.

Keywords: Free linear vibrations; Arbitrarily sagged inclined cables; Viscous fluid; Heavy fluid loading; Modal added mass; Modal damping coefficient

1. Introduction

Vibrations of cables in linear and nonlinear range have attracted considerable interest over the last few decades. The main features of linear vibrations of small sag horizontal or inclined suspended cables in air are by now well established (Irvine and Caughey, 1974; Irvine, 1981; Triantafyllou and Grinfogel, 1986), with a few articles still clarifying some relevant technical aspects (Russell and Lardner, 1998; Wu et al., 2005), whereas a number of comprehensive review articles have recently summarised the status of knowledge as regards nonlinear vibrations of small sag horizontal cables in air (Rega, 2004a, b) or in a flowing fluid (Ibrahim, 2004). Present research in the field is mostly devoted to the nonlinear analysis of larger sag and/or inclined cables (Zheng et al., 2002; Srinil et al., 2003, 2004, 2007), possibly based on improved cable modelling (Der Kiureghian and Sackman, 2005) and with increasing interest towards the analysis of interaction problems (Chang et al., 1997; Hu and Jin, 2001).

As regards the last issue, the effects of the interaction between a fluid and a submerged cable have been studied in connection with flow-induced effects (Ibrahim, 2004). Cable dynamics in water is indeed flow-induced when the cable is

*Corresponding author. Tel.: +45 9635 9332; fax: +45 9815 1675.
E-mail address: svs@ime.aau.dk (S.V. Sorokin).

0889-9746/$ - see front matter
doi:10.1016/j.jfluidstructs.2007.04.001

exposed to, e.g., the excitation due to transportation of a connected submerged device by a vessel. For a 'stationary' (i.e., suspended under water) cable, it makes more sense to consider the 'conventional' excitation exerted, for example, by external driving forces in a quiescent fluid. Apparently, such a problem formulation for the cable in water is more realistic than for the cable in air, because unsteady (e.g., wind-induced) excitation is typical for air rather than for water. The complete analytical description of the dynamics of a submerged cable is obviously more difficult than in air. The 'source' of such a complexity lies in the fact that the fluid–structure interaction should be considered in the coupled formulation (this is the so-called case of 'a structure under heavy fluid loading'). This formulation, in essence, suggests that the problems in fluid dynamics and structural dynamics must be solved simultaneously, rather than in a sequential (no feedback) manner. This concept is widely used in the analysis of other fluid–structure interaction problems, for example, in vibro-acoustics of naval structures (Junger and Feit, 1993).

The absence of a reasonably simple and meaningful theory to meet this challenge in the general case of large structural deflections and arbitrary regime of fluid motion stimulates researchers on this subject to utilise some empirical formulas, e.g., Morison's formula (Morison et al., 1950) to express the forces exerted on a cable by a flowing fluid. Simultaneously, the feedback influence of structural vibrations on fluid motion is ignored. In this formulation of the problem, when the essentially nonlinear behaviour of a fluid (which, unlike the case of wind-induced vibrations in air, must include the structural feedback) is described in a fairly approximate manner, it is doubtful how practical the detailed analysis of the nonlinear motion of a cable could be. As is well known, nonlinear phenomena are brought to light mostly in resonant excitation conditions. Moreover, the extent to which they are developed is actually controlled by the level of linear damping of the involved modes and by the presence of internal resonances in the model. Then, it is fairly obvious that, if the linear problem of vibrations of a cable in water is solved in a relatively poor manner, then all ensuing nonlinear analysis should be regarded as being aimed at merely qualitative rather than quantitative results.

Thus, it appears suitable to deal with vibrations of cables in water starting with the formulation of a consistent linear theory, to be subsequently exploited for the analysis of nonlinear vibrations, in the framework of the heavy fluid loading concept. In the realistic frequency range, this classical concept should be modified by ignoring the compressibility effects in water, but accounting for fluid viscosity. Naturally, the amplitudes of vibrations of a cable and the related fluid motion are assumed to be small enough to apply linear theory, and the mean flow in a fluid is set to zero. To the best of the authors' knowledge, such a problem formulation has not yet been explored in the literature, and this paper is aimed at solving this problem and yielding the physical interpretation of the obtained results.

Before addressing the vibration problem, it is necessary to determine the static equilibrium configuration of a suspended cable under its own weight (hereafter it is assumed that the cable does not bear any concentrated masses and/or dampers) (Irvine, 1981). In most publications, cables with relatively small sag are considered, for which the equilibrium shape is adequately captured by an elementary parabolic approximation. In some publications the extensibility of the cable axis is also taken into account. From the physical point of view it is fairly obvious that these two hypotheses are actually coupled. Indeed, in the limit case of a 'tight string' the equilibrium shape tends to the form of a straight line and the elastic elongation of the cable becomes important. In turn, the parabolic approximation of the equilibrium configuration of an almost straight cable is very satisfactory. If a cable with an arbitrarily large sag is considered, then both these hypotheses become questionable. The cable axis may be considered as inextensible, and the cable equilibrium shape may substantially deviate from the parabolic configuration, so that a catenary should be used to describe it. In some situations, the simplest model of inextensible cable of parabolic shape can be used.

The paper is structured as follows. In Section 2, the proper selection of a model to determine the static equilibrium shape of an arbitrarily sagged inclined cable in vacuum is addressed as a prerequisite for the analysis of cable vibrations in a quiescent fluid. Alternative analytical models are considered, and the relevant predictions are compared with each other and with a numerical solution in terms of static equilibrium configuration and natural frequencies. The central part of the paper is presented in Section 3, which is concerned with the derivation of coupled equations of linear vibrations of a cable and a surrounding viscous fluid. The theory developed in this section is applied in Section 4 to explore the influence of viscous fluid on eigenfrequencies of cables, modal added mass and modal damping coefficients, with the cable parameters already introduced in Section 2. A summary of results is reported in Section 5, where some directions for further research are also outlined.

2. A model of an arbitrarily sagged inclined cable and its validation

In this section, static equilibrium configurations and vibration features of a suspended inclined cable are obtained analytically by considering and comparing various models. It is advantageous to use a solution of the static equilibrium problem in closed analytical form because the vibration problem may then be easily solved by use of classical, e.g., Galerkin methods. The details of the analytical solution of an elastic catenary are available in Merkin (1980) and Irvine

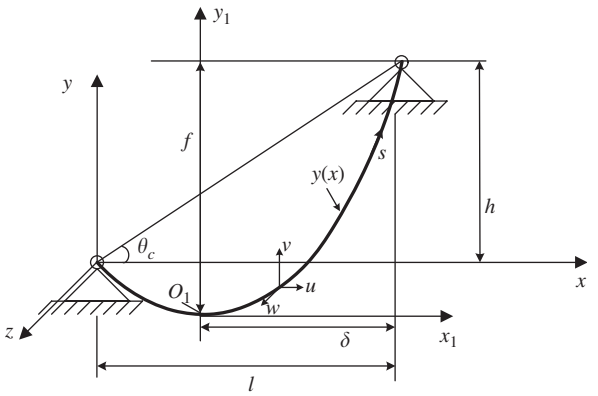

Fig. 1. A suspended cable—definitions and notations.

(1981). The following notations are used (Fig. 1): l is the horizontal span, h is the height difference between supports ($\theta_C = \arctan(h/l)$), δ and f are the (dimensional) coordinates of the right support in the system of coordinates $O_1x_1y_1$ with the origin in the lowest point of the cable. The solution of the extensible catenary (Merkin, 1980) reads

$$x_1 = \frac{H}{q_0}\left[\chi + \frac{H}{EA}\sinh\chi\right] + C_1, \quad y_1 = \frac{H}{q_0}\left[\cosh\chi + \frac{1}{2}\frac{H}{EA}\cosh^2\chi\right] + C_2, \tag{1}$$

where H is the horizontal component of the tension force T, $q_0 = \rho g A$ is the gravitational force per unit cable length before stretching, E, ρ, and A are the Young modulus, the cable mass density, and the area of the cross-section, and $\chi \equiv \ln\tan\left((\pi/4) + (\alpha/2)\right)$, with the angle α denoting the cable local slope. The parameters C_1 and C_2 are defined by the suspension conditions at the left edge of the cable ($\chi = \chi_1$), whereas the suspension condition at the right edge ($\chi = \chi_2$) yields

$$\chi_2 - \chi_1 + \frac{H}{EA}(\sinh\chi_2 - \sinh\chi_1) = \frac{lq_0}{H}, \tag{2a}$$

$$\cosh\chi_2 - \cosh\chi_1 + \frac{1}{2}\frac{H}{EA}(\cosh^2\chi_2 - \cosh^2\chi_1) = \frac{hq_0}{H}. \tag{2b}$$

One more equation is given by the equilibrium condition

$$\sinh\chi_2 - \sinh\chi_1 = \frac{L_0 q_0}{H}, \tag{2c}$$

where L_0 is the undeformed cable length.

The system of nonlinear Eqs. (2a)–(2c) with respect to H, χ_1 and χ_2 is easily solved numerically for any combination of parameters, furnishing the explicit solution of the extensible catenary in the parametric form (1).

By setting $EA \to \infty$ and $L = L_0$, with L being the cable length in the deformed (equilibrium) configuration, the solution for the inextensible catenary (chain line) in the Oxy system is obtained

$$y(x) = \frac{H}{q_0}\left\{\cosh\left[\frac{q_0 l}{H}\left(\frac{x}{l} - 1 + \frac{\delta}{l}\right)\right] - 1\right\} - f + h. \tag{3}$$

A simplified formulation of this solution utilises a two-term approximation of the hyperbolic cosine function that yields

$$y(x) = x\tan\theta_C - \frac{1}{2}x\left(1 - \frac{x}{l}\right)\frac{q_0 l}{H}\left\{1 - \frac{1}{6}\left(1 - 2\frac{x}{l}\right)\frac{q_0 l}{H}\sin\theta_C\right\}\frac{1}{\cos\theta_C}. \tag{4}$$

Accounting for extensibility, the dimensional equations of free nonlinear vibrations of an inclined cable read (Srinil et al., 2003)

$$\left[\frac{EA(1+\tilde{u}') + T\tilde{u}'}{\sqrt{1+(y')^2}} - \frac{EA(1+\tilde{u}')}{\sqrt{(1+\tilde{u}')^2 + (y'+\tilde{v}')^2 + (\tilde{w}')^2}}\right]' = \sqrt{1+(y')^2}\rho A\ddot{\tilde{u}}\left(1 + \frac{T}{EA}\right)^{-1}, \tag{5a}$$

$$\left[\frac{EA(y'+\tilde{v}')+T\tilde{v}'}{\sqrt{1+(y')^2}}-\frac{EA(y'+\tilde{v}')}{\sqrt{(1+\tilde{u}')^2+(y'+\tilde{v}')^2+(\tilde{w}')^2}}\right]'=\sqrt{1+(y')^2}\rho A\ddot{\tilde{v}}\left(1+\frac{T}{EA}\right)^{-1}, \tag{5b}$$

$$\left[\frac{EA\tilde{w}'+T\tilde{w}'}{\sqrt{1+(y')^2}}-\frac{EA\tilde{w}'}{\sqrt{(1+\tilde{u}')^2+(y'+\tilde{v}')^2+(\tilde{w}')^2}}\right]'=\sqrt{1+(y')^2}\rho A\ddot{\tilde{w}}\left(1+\frac{T}{EA}\right)^{-1}, \tag{5c}$$

where the displacement components $\tilde{u}$ and $\tilde{v}$ describe in-plane vibrations of the cable, whereas $\tilde{w}$ is the out-of-plane displacement component, see Fig. 1. The standard notations of primes and dots designate derivatives with respect to spatial and temporal coordinates. The static tension force for the inextensible catenary is

$$T(x)=H\left\{\cosh\left[\frac{q_0 l}{H}\left(\frac{x}{l}-1+\frac{\delta}{l}\right)\right]-1\right\}. \tag{6}$$

In this paper, small-amplitude cable vibrations in a viscous fluid are considered so that Eqs. (5) are linearised

$$\frac{T\tilde{u}''}{\sqrt{1+(y')^2}}+\left[\frac{EA}{\sqrt{1+(y')^2}}(\tilde{u}'+y'\tilde{v}')\right]'=\sqrt{1+(y')^2}\rho A\ddot{\tilde{u}}\left(1+\frac{T}{EA}\right)^{-1}+f_X, \tag{7a}$$

$$\frac{T\tilde{v}''}{\sqrt{1+(y')^2}}+\left[\frac{EA}{\sqrt{1+(y')^2}}\left(y'\tilde{u}'+(y')^2\tilde{v}'\right)\right]'=\sqrt{1+(y')^2}\rho A\ddot{\tilde{v}}\left(1+\frac{T}{EA}\right)^{-1}+f_Y, \tag{7b}$$

$$\frac{T\tilde{w}''}{\sqrt{1+(y')^2}}=\sqrt{1+(y')^2}\rho A\ddot{\tilde{w}}\left(1+\frac{T}{EA}\right)^{-1}+f_Z \tag{7c}$$

and the components (f_X, f_Y, f_Z) of the force exerted by a fluid are added to the right-hand sides. These forces will be found in Section 3 by solving the 'fluid' part of the coupled problem.

Before addressing the vibration problem in water, the validity ranges of the three considered cable models, namely (i) the exact *extensible catenary*, obtained numerically from Eqs. (1) and (2), (ii) the exact analytical *inextensible catenary* (Eq. (3)), and (iii) its *cubic approximation* (Eq. (4)), are evaluated by comparing the static equilibrium configurations and the eigenfrequencies of cable vibrations without fluid loading effect taken into account.

The parameters of an inclined cable are $l=850\,\mathrm{m}$, $A=0.1159\,\mathrm{m}^2$, $\rho=8337.9\,\mathrm{kg/m}^3$, and $E=1.794.10^8\,\mathrm{kN/m}^2$. Following (Srinil et al., 2003), three configurations defined by the angles $\theta_C=\frac{1}{6}\pi$, $\theta_C=\frac{1}{4}\pi$ and $\theta_C=\frac{1}{3}\pi$ are selected. For each of them, three increasing values of undeformed cable length are considered (see Table 1 forward), starting from the value corresponding to second avoidance in the in-plane frequency spectrum.

Analysis of the equilibrium configurations obtained with the three models shows that the extensible and inextensible catenary shapes are nearly undistinguishable from each other for all of the considered values of angle of inclination and of undeformed cable length. This does not appear surprising, since it confirms—in various parameter ranges—the practical negligibility of cable extensibility in the static problem, already known from the literature: indeed, its influence is simply that the effective length of the cable is greater than the original one (Irvine, 1981). Thus, the inextensible catenary can be usefully assumed as a closed-form cable equilibrium solution in further investigations. However, its cubic approximation provides results that, while being quite accurate for the lower considered values of cable length, become less accurate as the angle θ_C increases and/or the length increases. The differences between the "exact" (continuous curve) and approximate (dashed curve) inextensible catenary shapes are shown in Fig. 2 for the maximum value of cable length considered at each of the three inclination angles. This is also not entirely surprising since the considered L_0 values correspond to very high sag-to-span ratios, where also the cubic approximation—besides the parabolic one—is expected to fail. Practically, it may be concluded that the cubic approximation fails as soon as the lower suspension point ceases to be the lowest point of the whole cable.

Additional insight into the matter is given by comparing the eigenfrequencies and eigenmodes of vibrations of a cable in vacuum, as obtained with the two—exact versus approximate—inextensible catenary models $y(x)$. In each case, the set of eigenfrequencies and eigenmodes is found from the system of Eq. (7) with the fluid loading terms omitted.

Table 1
Eigenfrequencies (Hz) of a cable with different inclination angles and lengths, vibrating in vacuum

Inclination angle (θ_c)	Cable length L (m)	Cable model	Out-of-plane (1st)	Out-of-plane (2nd)	In-plane (1st)	In-plane (2nd)
$\pi/6$	987.8	Srinil et al. (2003)	0.074	0.148	0.146	0.202
		Exact	0.0743	0.148	0.148	0.206
		Approximate	0.0743	0.148	0.148	0.206
	1187.8	Exact	0.0309	0.0593	0.0525	0.110
		Approximate	0.0320	0.0619	0.0542	0.103
	1387.8	Exact	0.0258	0.0480	0.0395	0.0921
		Approximate	0.0288	0.0544	0.0443	0.0856
$\pi/4$	1209.9	Srinil et al. (2003)	0.060	0.121	0.118	0.165
		Exact	0.0606	0.121	0.120	0.168
		Approximate	0.0606	0.121	0.120	0.168
	1409.9	Exact	0.0273	0.0532	0.0450	0.0918
		Approximate	0.0278	0.0546	0.0449	0.0823
	1609.9	Exact	0.0233	0.0442	0.0346	0.0787
		Approximate	0.0248	0.0481	0.0378	0.0792
$\pi/3$	1711.0	Srinil et al. (2003)	0.043	0.086	0.082	0.117
		Exact	0.0431	0.0861	0.0830	0.119
		Approximate	0.0431	0.0861	0.0829	0.120
	1911.0	Exact	0.0222	0.0438	0.0346	0.0682
		Approximate	0.0216	0.0441	0.0336	0.0643
	2111.0	Exact	0.0194	0.0379	0.0276	0.0600
		Approximate	0.0185	0.0381	0.0299	0.0650

The time dependence is introduced through the separate variable approximation as

$$\tilde{u}(x,t) = u(x)\exp(-\mathrm{i}\omega t), \quad \tilde{v}(x,t) = v(x)\exp(-\mathrm{i}\omega t), \quad \tilde{w}(x,t) = w(x)\exp(-\mathrm{i}\omega t). \tag{8}$$

Furthermore, the standard Galerkin method is applied with a few terms retained

$$u(x) = \sum_{m=1}^{M_u} A_m \sin\frac{m\pi x}{L}, \quad v(x) = \sum_{m=1}^{M_v} B_m \sin\frac{m\pi x}{L}, \quad w(x) = \sum_{m=1}^{M_w} C_m \sin\frac{m\pi x}{L}. \tag{9}$$

Then the frequency determinant is formulated as a polynomial of order $M_u + M_v + M_w$ with respect to ω^2 and all its roots can be easily found by use of, say, *Mathematica* (Wolfram, 1991).

The frequencies in Hz obtained for $M_u + M_v + M_w = 5$ are summarised in Table 1, which allows us to make some worthwhile conclusions. First, the Galerkin approximation of vibration shape with a relatively small number of terms is sufficiently accurate to determine the first two eigenfrequencies of out-of-plane and in-plane spectra. There is a very small difference between them and the results obtained in Srinil et al. (2003) by using a detailed finite element model, also reported for comparison whenever possible. Of course, one should retain more terms in (9) to determine the eigenfrequencies of higher order modes (Srinil et al., 2007). Second, the agreement between exact and approximate models is excellent in all cases when the difference between the static configurations is vanishingly small. The discrepancy becomes larger as the cable length increases, and the eigenfrequencies predicted by the approximate model deviate from those obtained with the exact formulation in up to 10–15%.

Further comparison is related to the eigenmodes of vibrations for the case $\theta_C = \frac{1}{3}\pi$ (the highest inclination angle) with either low ($L_0 = 1711$ m) or high ($L_0 = 2111$ m) value of cable length. The mode shapes of the former, as obtained with the exact (continuous) and approximate (dashed) models, are shown in Figs. 3 and 4 in a normalised system reference. Fig. 3(a) and (b) presents the first and second out-of-plane modes, whereas Fig. 4(a) and (b) presents the same results for in-plane motions, distinguishing between the horizontal $u(x)$ (thin) and vertical $v(x)$ (thick) displacement components. As expected, there is no difference in the mode shapes, and orthogonality conditions hold for each set.

The mode shapes of out-of-plane and in-plane vibrations of the high length case are shown in Figs. 5 and 6. Results obtained by use of the exact model are in continuous thin ($u(x)$, $w(x)$) and thick ($v(x)$), those obtained by use of approximate model are shown in dashed thin ($u(x)$, $w(x)$) and thick ($v(x)$). There is a significant difference between the

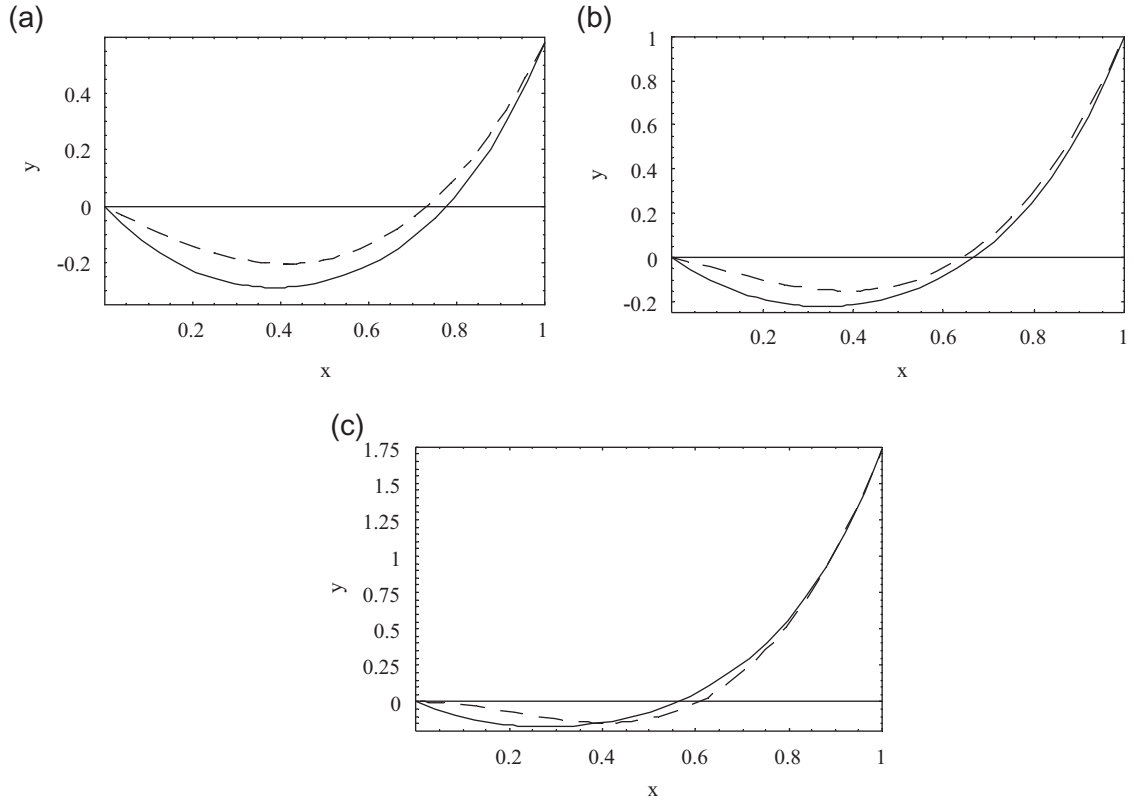

Fig. 2. Static equilibrium configurations of a cable with exact (continuous) or approximate (dashed) catenary models. (a): $\theta_C = \pi/6$, $L_0 = 1387.8$ m; (b): $\theta_C = \pi/4$, $L_0 = 1609.9$ m; (c) $\theta_C = \pi/3$, $L_0 = 2111$ m (coordinates are scaled by l).

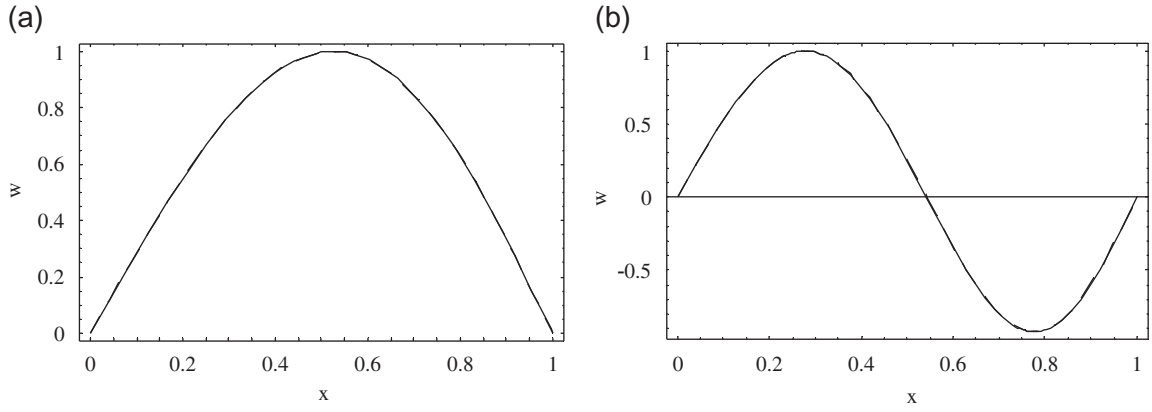

Fig. 3. (a) The first and (b) the second out-of-plane modes $\theta_C = \pi/3$, $L_0 = 1711$ m.

predictions of the two models, in particular for the in-plane vibrations. This difference is expected to be important also in the analysis of cable vibrations into water, mostly as regards the effects associated with the more pronounced axial components displacement highlighted by the exact model.

Summarising, one can say that, while there is no need to account for cable extensibility, the closed-form *exact* solution of the *inextensible catenary* has to be used as the static equilibrium configuration, instead of the approximate solution, in the subsequent investigation of cable dynamics in water. In this respect, even the exact model allows one to

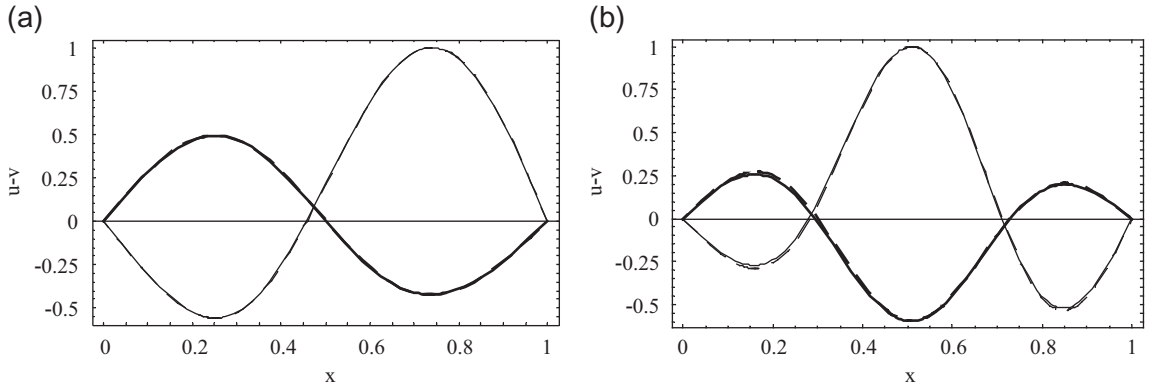

Fig. 4. (a) The first and (b) the second in-plane modes $\theta_C = \pi/3$, $L_0 = 1711$ m.

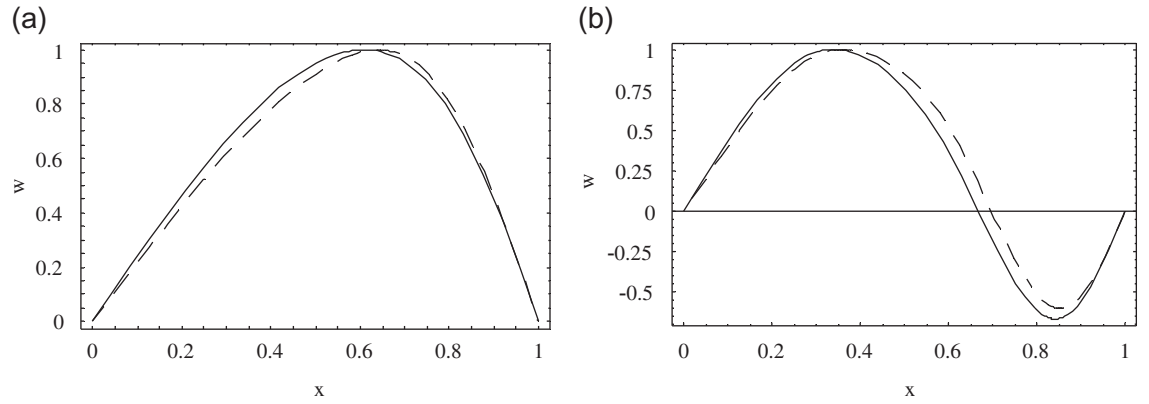

Fig. 5. (a) The first and (b) the second out-of-plane modes $\theta_C = \pi/3$, $L_0 = 2111$ m.

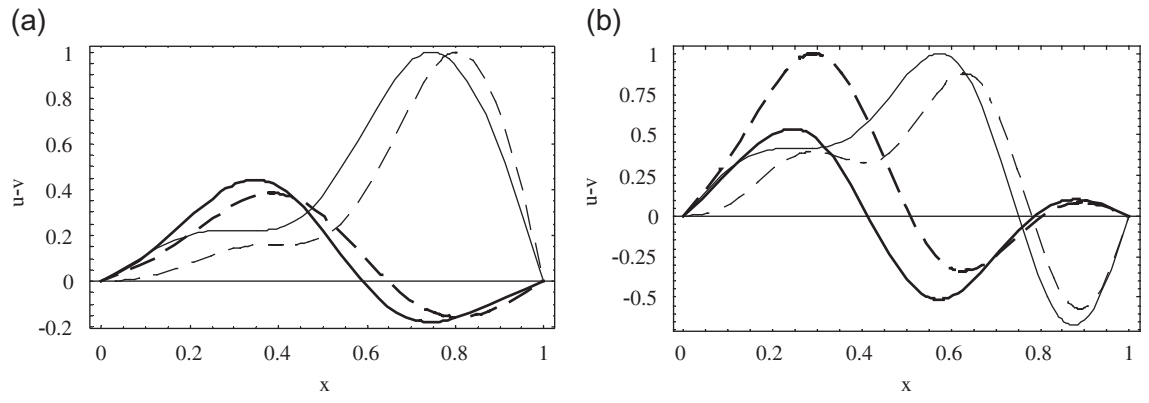

Fig. 6. (a) The first and (b) the second in-plane modes $\theta_C = \pi/3$, $L_0 = 2111$ m.

pursue the solution of the vibration problem governed by Eq. (5) with the function $y(x)$ being given in explicit analytic form, thus being very useful. It is worth noticing that the inextensibility assumption herein made as regards the statics of the problem will no more be used when studying the dynamics (Irvine, 1981).

3. A model of interaction between a cable and a quiescent viscous fluid

When dealing with vibrations of cables submerged in a fluid (e.g., water), the fluid–structure interaction effects play an important role. The standard formulation of the problem addresses the case of flow-induced vibrations (Ibrahim, 2004), when the equilibrium configuration is affected by mean flow effects and the perturbations of the mean flow provoke its motion. Actually, the coupled problem of large amplitude nonlinear vibrations of a cable in a flowing fluid is extremely complicated and the satisfactory theoretical model is yet to be developed. Therefore, a common approach to model this interaction is based on using some empirical or semi-empirical formulas [e.g., the Morison equation, see Ibrahim (2004)] for evaluating the force exerted by a fluid on the cable.

However, in contrast with cable dynamics in air, where wind-induced vibrations are the most 'natural' excitation conditions, cable dynamics in water may be regarded as being flow-induced mostly if the cable is exposed to the excitation due to transportation of a connected submerged device by a vessel. For a 'stationary' (i.e., suspended under water) cable, it makes more sense to consider the 'conventional' excitation exerted, for example, by external driving forces in a quiescent fluid. Then the coupled problem in fluid–structure interaction becomes relatively simple and this interaction may be modelled theoretically. The ultimately simple model of such an interaction is readily available as the added mass concept. However, this approximation does not take into account the damping properties of water and its frequency-dependent inertia.

When vibrations of a cable occur in a quiescent fluid, it is possible to formulate a consistent theoretical model and to express the forces exerted on the cable analytically via components of cable velocities. This theory includes the linearised equations of cable motion (5) around its static equilibrium configuration, the linearised Navier–Stokes equations of motion of a viscous fluid (in the low-frequency excitation regime the role of compressibility is known to be negligible) and the continuity conditions of velocities at the cable surface in its static configuration. Furthermore, it is reasonable to assume slenderness of the cable, because even in the case of a very large static deflection, the ratio ε of the radius of its cross-section R to the minimum radius of curvature of its axis R_0 is of order $\varepsilon\sim10^{-4}$. This entails that, locally, the cable may be considered as being of cylindrical shape, and that the local fluid dynamics may be described in the frame of cylindrical coordinates by using the asymptotic formulation of Navier–Stokes equations in powers of the small parameter ε. Thus, the continuity and Navier–Stokes equations are formulated as (Landau and Livshitz, 1987; Milne-Thompson, 1988)

$$\frac{1}{r}\frac{\partial(rV_r)}{\partial r}+\frac{1}{r}\frac{\partial V_\theta}{\partial\theta}+\frac{\partial V_x}{\partial x}=0, \tag{10a}$$

$$\frac{\partial V_r}{\partial t}=-\frac{1}{\rho_{fl}}\frac{\partial p}{\partial r}+\nu_{fl}\left(\Delta V_r-\frac{2}{r^2}\frac{\partial V_\theta}{\partial\theta}-\frac{V_r}{r^2}\right), \tag{10b}$$

$$\frac{\partial V_\theta}{\partial t}=-\frac{1}{\rho_{fl}r}\frac{\partial p}{\partial\theta}+\nu_{fl}\left(\Delta V_\theta+\frac{2}{r^2}\frac{\partial V_r}{\partial\theta}-\frac{V_\theta}{r^2}\right), \tag{10c}$$

$$\frac{\partial V_x}{\partial t}=-\frac{1}{\rho_{fl}}\frac{\partial p}{\partial x}+\nu_{fl}\Delta V_x. \tag{10d}$$

Here (V_r,V_θ,V_x) are velocity components, p is the pressure, ρ_{fl} and ν_{fl} are fluid density and kinematic viscosity. As already mentioned, the cylindrical coordinates (the radial coordinate r is counted from the centre of cable's cross-section, the circumferential coordinate θ is counted from the vertical coordinate y anticlockwise) are introduced because the cable is sufficiently slender and the hydrodynamics of fluid motion generated by vibrations of each cable segment may be described as if it were cut from an infinitely long cylindrical body. To be more precise, Eq. (10) should be written in the coordinates (s,r,θ), where the globally curvilinear s-axis is directed along the cable. However, cable slenderness permits one to locally consider this axis as a perturbed straight one and to apply the asymptotic formulation of Navier–Stokes equations in powers of a small parameter ε. Then the leading-order contribution corresponds to vibrations of an ideally straight cylindrical body in a viscous fluid. For calculation purposes, this straight body could be considered as unboundedly extended along the overall chord of the cable's equilibrium configuration and the x-axis introduced in Eq. (10) as co-directed with this chord.

Although it does not present serious difficulties to proceed with Eq. (10), their solution is easier if velocity components are expressed in terms of three velocity potentials $\tilde{\varphi}$, $\tilde{\psi}_1$, $\tilde{\psi}_2$ as (Guz, 1981; Kadyrov, Wauer and Sorokin, 2001)

$$V_r = \frac{\partial\tilde{\varphi}}{\partial r} + \frac{1}{r}\frac{\partial\tilde{\psi}_1}{\partial\theta} + \frac{\partial^2\tilde{\psi}_2}{\partial r\partial x}, \quad V_\theta = \frac{1}{r}\frac{\partial\tilde{\varphi}}{\partial\theta} - \frac{\partial\tilde{\psi}_1}{\partial r} + \frac{1}{r}\frac{\partial^2\tilde{\psi}_2}{\partial\theta\partial x}, \quad V_x = \frac{\partial\tilde{\varphi}}{\partial x} + \Delta\tilde{\psi}_2 - \frac{\partial^2\tilde{\psi}_2}{\partial x^2}. \tag{11}$$

A similar presentation of solution is often used in the theory of elasticity. The pressure is defined as

$$p = -\rho_{fl}\frac{\partial\tilde{\varphi}}{\partial t}. \tag{12}$$

Substitution of formulas (11)–(12) into Eq. (10) and elementary transformations yield a system of three uncoupled differential equations with respect to velocity potentials

$$\frac{\partial^2\tilde{\varphi}}{\partial r^2} + \frac{1}{r}\frac{\partial\tilde{\varphi}}{\partial r} + \frac{1}{r^2}\frac{\partial^2\tilde{\varphi}}{\partial\theta^2} + \frac{\partial^2\tilde{\varphi}}{\partial x^2} = 0, \tag{13a}$$

$$\frac{\partial^2\tilde{\psi}_1}{\partial r^2} + \frac{1}{r}\frac{\partial\tilde{\psi}_1}{\partial r} + \frac{1}{r^2}\frac{\partial^2\tilde{\psi}_1}{\partial\theta^2} + \frac{\partial^2\tilde{\psi}_1}{\partial x^2} - \frac{1}{v_{fl}}\frac{\partial\tilde{\psi}_1}{\partial t} = 0, \tag{13b}$$

$$\frac{\partial^2\tilde{\psi}_2}{\partial r^2} + \frac{1}{r}\frac{\partial\tilde{\psi}_2}{\partial r} + \frac{1}{r^2}\frac{\partial^2\tilde{\psi}_2}{\partial\theta^2} + \frac{\partial^2\tilde{\psi}_2}{\partial x^2} - \frac{1}{v_{fl}}\frac{\partial\tilde{\psi}_2}{\partial t} = 0. \tag{13c}$$

The boundary conditions at the cable surface, $r = R$, are:

$$\frac{\partial\tilde{\varphi}}{\partial r} + \frac{1}{r}\frac{\partial\tilde{\psi}_1}{\partial\theta} + \frac{\partial^2\tilde{\psi}_2}{\partial r\partial x} = \frac{\partial\tilde{w}}{\partial t}\sin\theta + \frac{\partial\tilde{v}}{\partial t}\cos\theta, \tag{14a}$$

$$\frac{1}{r}\frac{\partial\tilde{\varphi}}{\partial\theta} - \frac{\partial\tilde{\psi}_1}{\partial r} + \frac{1}{r}\frac{\partial^2\tilde{\psi}_2}{\partial\theta\partial x} = \frac{\partial\tilde{w}}{\partial t}\cos\theta - \frac{\partial\tilde{v}}{\partial t}\sin\theta, \tag{14b}$$

$$\frac{1}{v_{fl}}\frac{\partial\tilde{\psi}_2}{\partial t} = -\frac{\partial\tilde{u}}{\partial t}. \tag{14c}$$

As is seen, the three velocity potentials remain coupled via the boundary conditions (note that the measure of $\tilde{\varphi}$ and $\tilde{\psi}_1$ is $\mathrm{m}^2\,\mathrm{s}^{-1}$, whereas $\tilde{\psi}_2$ is measured by $\mathrm{m}^3\,\mathrm{s}^{-1}$).

The stresses in the viscous fluid are defined by the formulas

$$\tilde{\sigma}_{rr} = 2\rho_{fl}v_{fl}\left\{\left[\frac{1}{2v_{fl}}\frac{\partial}{\partial t} - \frac{\partial^2}{\partial x^2} - \frac{1}{r}\frac{\partial}{\partial r} - \frac{1}{r^2}\frac{\partial^2}{\partial\theta^2}\right]\tilde{\varphi} + \frac{\partial^2}{\partial r\partial\theta}\left[\frac{1}{r}\tilde{\psi}_1\right] + \frac{\partial}{\partial x}\left[\frac{1}{v_{fl}}\frac{\partial}{\partial t} - \frac{\partial^2}{\partial x^2} - \frac{1}{r}\frac{\partial}{\partial r} - \frac{1}{r^2}\frac{\partial^2}{\partial\theta^2}\right]\tilde{\psi}_2\right\}, \tag{15a}$$

$$\tilde{\tau}_{r\theta} = 2\rho_{fl}v_{fl}\left\{\frac{\partial^2}{\partial r\partial\theta}\left[\frac{1}{r}\tilde{\varphi}\right] + \left[-\frac{1}{2v_{fl}}\frac{\partial}{\partial t} + \frac{1}{2}\frac{\partial^2}{\partial x^2} + \frac{1}{r}\frac{\partial}{\partial r} + \frac{1}{r^2}\frac{\partial^2}{\partial\theta^2}\right]\tilde{\psi}_1 + \frac{\partial^3\tilde{\psi}_2}{r\partial x\partial r\partial\theta}\right\}, \tag{15b}$$

$$\tilde{\tau}_{rx} = 2\rho_{fl}v_{fl}\left\{\frac{\partial^2\tilde{\varphi}}{\partial r\partial x} + \frac{1}{2}\frac{1}{r}\frac{\partial^2\tilde{\psi}_1}{\partial x\partial\theta} + \frac{\partial}{\partial r}\left[\frac{\partial^2}{\partial x^2} - \frac{1}{2v_{fl}}\frac{\partial}{\partial t}\right]\tilde{\psi}_2\right\}. \tag{15c}$$

Eqs. (13) are derived under the assumption that the cable is sufficiently slender. It is consistent to pursue this assumption further and to decouple two components of fluid motion: the in-plane one (with reference to the cable cross-section) and the anti-plane one (i.e., the sliding longitudinal motion along the x-axis).

The potentials $\tilde{\varphi}$ and $\tilde{\psi}_1$ are assumed to be independent of the axial coordinate x

$$\tilde{\varphi}(r,\theta,t) = \tilde{\varphi}_w(r,t)\sin\theta + \tilde{\varphi}_v(r,t)\cos\theta, \quad \tilde{\psi}_1(r,\theta,t) = -\tilde{\psi}_{1w}(r,t)\cos\theta + \tilde{\psi}_{1v}(r,t)\sin\theta. \tag{16}$$

Physically, this means that no fluid flow along the axis of the cable is generated by its oscillations in the plane of cross-section.

The axial component of fluid motion, which is relevant to pure sliding of the cable (modelled as an infinitely long straight cylinder) is captured by the potential $\tilde{\psi}_2$ regarded as being independent of both the circumferential and the axial coordinate

$$\tilde{\psi}_2(r,\theta,t) = \tilde{\psi}_{2u}(r,t). \tag{17}$$

In effect, simplifications (16) and (17) mean that each cable cross-section is involved in a pure transversal motion, in which fluid particles do not move along the rod axis (this motion is referred to as in-plane 'cross-axis'), and in a pure axial motion, in which fluid particles uniformly move along the rod axis (this motion is referred to as anti-plane 'sliding', see standard texts in the theory of elasticity). Thus, both the in-plane and anti-plane motions are captured, but their interaction is ignored. It is anticipated that the error introduced by use of this model is of the same (or lower) order of magnitude than the error already introduced by retaining just the leading order term in the expansion on the slenderness parameter ε.

Small amplitude linear vibrations of the cable are considered, so that all of the introduced functions are given the same time dependence of $\exp(-\mathrm{i}\omega t)$, e.g., $\tilde{\varphi}_w(r,t) = \varphi_w(r)\exp(-\mathrm{i}\omega t)$. Then Eqs. (13) and (14) are reduced to three sets of uncoupled problems governing:

(i) *cable vibrations out of the plane of equilibrium configuration*

$$\frac{\mathrm{d}^2\varphi_w}{\mathrm{d}r^2}+\frac{1}{r}\frac{\mathrm{d}\varphi_w}{\mathrm{d}r}-\frac{1}{r^2}\varphi_w=0,\quad \frac{\mathrm{d}^2\psi_{1w}}{\mathrm{d}r^2}+\frac{1}{r}\frac{\mathrm{d}\psi_{1w}}{\mathrm{d}r}-\frac{1}{r^2}\psi_{1w}+\frac{\mathrm{i}\omega}{v_{fl}}\psi_{1w}=0,$$

$$r=R:\quad \frac{\mathrm{d}\varphi_w}{\mathrm{d}r}+\frac{1}{r}\psi_{1w}=-\mathrm{i}\omega w,\quad \frac{1}{r}\varphi_w+\frac{\mathrm{d}\psi_{1w}}{\mathrm{d}r}=-\mathrm{i}\omega w. \tag{18}$$

(ii) *cable vibrations in the plane of equilibrium configuration*

$$\frac{\mathrm{d}^2\varphi_v}{\mathrm{d}r^2}+\frac{1}{r}\frac{\mathrm{d}\varphi_v}{\mathrm{d}r}-\frac{1}{r^2}\varphi_v=0,\quad \frac{\mathrm{d}^2\psi_{1v}}{\mathrm{d}r^2}+\frac{1}{r}\frac{\mathrm{d}\psi_{1v}}{\mathrm{d}r}-\frac{1}{r^2}\psi_{1v}+\frac{\mathrm{i}\omega}{v_{fl}}\psi_{1v}=0,$$

$$r=R:\quad \frac{\mathrm{d}\varphi_v}{\mathrm{d}r}+\frac{1}{r}\psi_{1v}=-\mathrm{i}\omega v,\quad \frac{1}{r}\varphi_v+\frac{\mathrm{d}\psi_{1v}}{\mathrm{d}r}=-\mathrm{i}\omega v. \tag{19}$$

(iii) *anti-plane sliding vibrations*

$$\frac{\mathrm{d}^2\psi_{2u}}{\mathrm{d}r^2}+\frac{1}{r}\frac{\mathrm{d}\psi_{2u}}{\mathrm{d}r}+\frac{\mathrm{i}\omega}{v_{fl}}\psi_{2u}=0,$$

$$r=R:\quad \frac{\mathrm{i}\omega}{v_{fl}}\psi_{2u}=-\mathrm{i}\omega u. \tag{20}$$

The normal and shear stresses are determined from formulas (15) and their resultants are substituted into equations of cable motion (7).

The solution of problem (18) reads

$$\varphi_w=\frac{\mathrm{i}\omega wR^2}{r}\left(1-\frac{2}{\eta}\right),\quad \psi_{1w}=-2\mathrm{i}\omega wR\frac{1}{\eta}\frac{\mathrm{H}_1^{(1)}\left(\sqrt{\mathrm{i}(\omega R^2/v_{fl})}(r/R)\right)}{\mathrm{H}_1^{(1)}\left(\sqrt{\mathrm{i}(\omega R^2/v_{fl})}\right)}, \tag{21}$$

$$\eta=1+\frac{1}{2}\sqrt{\mathrm{i}\frac{\omega R^2}{v_{fl}}}\frac{\mathrm{H}_0^{(1)}\left(\sqrt{\mathrm{i}(\omega R^2/v_{fl})}\right)-\mathrm{H}_2^{(1)}\left(\sqrt{\mathrm{i}(\omega R^2/v_{fl})}\right)}{\mathrm{H}_1^{(1)}\left(\sqrt{\mathrm{i}(\omega R^2/v_{fl})}\right)} \tag{22}$$

and H denotes a Hankel function. Then stresses (15) become

$$\sigma_{rr}^w=\rho_{fl}\omega^2 wR\left(1-\frac{2}{\eta}\right)\sin\theta,\quad \tau_{r\theta}^w=\rho_{fl}\omega^2 wR\frac{2}{\eta}\cos\theta. \tag{23}$$

Respectively, the force resultants (per unit length) in the in-plane and out-of-plane directions are

$$f_Y^w = \int_0^{2\pi} \left(-\sigma_{rr}^w \cos\theta + \tau_{r\theta}^w \sin\theta\right) R\mathrm{d}\theta = 0, \tag{24a}$$

$$f_Z^w = \int_0^{2\pi} \left(-\sigma_{rr}^w \sin\theta + \tau_{r\theta}^w \cos\theta\right) R\mathrm{d}\theta = -\rho_{fl}\omega^2 w\pi R^2\left(1-\frac{4}{\eta}\right). \tag{24b}$$

The formula for the component f_Z^w naturally merges the elementary formula for the added mass of an incompressible inviscid fluid as $v_{fl}\to 0$ so that $\eta\to\infty$. Strictly speaking, these forces are exerted by the fluid in normal and binormal directions to the axis of a curvilinear cable in its equilibrium configuration. However, within an acceptable tolerance level for linear dynamic analyses, these forces may be identified with those acting in the vertical and horizontal directions, respectively, and they are labelled this way.

Problem (19) is solved analogously and the force per unit length components produced in response to the in-plane motion are

$$f_Y^v = -\rho_{fl}\omega^2 v\pi R^2\left(1-\frac{4}{\eta}\right), \quad f_Z^v = 0. \tag{25}$$

Finally, the anti-plane problem has the following solution:

$$\psi_2 = -v_{fl}u\frac{\mathrm{H}_0^{(1)}\left(\sqrt{\mathrm{i}(\omega R^2/v_{fl})}(r/R)\right)}{\mathrm{H}_0^{(1)}\left(\sqrt{\mathrm{i}(\omega R^2/v_{fl})}\right)}. \tag{26}$$

Then the shear stress is

$$\tau_{rx} = \mathrm{i}\frac{\rho_{fl}v_{fl}\omega}{R}u\eta_1, \quad \eta_1 = \sqrt{\mathrm{i}\frac{\omega R^2}{v_{fl}}}\frac{\mathrm{H}_1^{(1)}\left(\sqrt{\mathrm{i}(\omega R^2/v_{fl})}\right)}{\mathrm{H}_0^{(1)}\left(\sqrt{\mathrm{i}(\omega R^2/v_{fl})}\right)}. \tag{27}$$

The axial force per unit length becomes

$$f_X^u = 2\pi\mathrm{i}\rho_{fl}v_{fl}\omega u\eta_1. \tag{28}$$

Formulas (24), (25) and (28) involve ratios of Hankel functions of a complex argument. Therefore, it is appropriate to explore a possibility to replace them by their asymptotic formulation. For definiteness, refer to the cable parameters specified in Section 2 and assume that vibrations in water are considered. The radius of cable cross-section is of order 10^{-1} m and the eigenfrequencies of its vibrations in vacuum are of order $10^{-1}\,\mathrm{s}^{-1}$, see Table 2. The kinematic viscosity of water is of order $10^{-5}\,\mathrm{m}^2\,\mathrm{s}^{-1}$. Then the argument of Hankel functions is of order 10 and it is possible to reduce formulas for η and η_1 to their asymptotics, which are very simple

$$\eta = 1+\mathrm{i}\sqrt{\mathrm{i}\frac{\omega R^2}{v_{fl}}}, \quad \eta_1 = \mathrm{i}\sqrt{\mathrm{i}\frac{\omega R^2}{v_{fl}}}. \tag{29}$$

It is a trivial task to show that the asymptotic formulas are perfectly valid provided the argument is not small. In the considered example (vibrations in water), small values of the argument refer to unrealistically low frequencies (of order 10^{-3} Hz), while the resonant frequencies of the cables reported in Table 2 lie within the range of applicability of the formulas.

To have a simple estimate of the contribution of viscosity of water towards the added mass and the damping of cable, it is appropriate to compare the force resultant exerted by an incompressible inviscid fluid on a rigid cylinder (the standard added mass model), which performs transverse oscillations, with the force given by formula (24b). Apparently, the sliding anti-plane vibrations of this cylinder are not resisted by the fluid at all. The elementary formula for the inertial force generated by an added mass in transverse motion is $f_0 = -\rho_{fl}\omega^2 w\pi R^2$. Then the contribution of viscosity is given by the factor $C = 1-(4/\eta)$. In Figs. 7(a) and (b) the added mass coefficient (i.e., the real part of C) and the viscous damping coefficient (i.e., the imaginary part of C) are shown versus frequency in Hertz. As is seen, viscosity increases the added mass and also produces rather significant damping (the imaginary part of the reaction force is about one order of magnitude smaller than its real part). Some reservations should be expressed as regards the physical meaning of these results. First, they are obtained by the linearised Navier–Stokes equations. Therefore, extrapolation of the curves in Fig. 7 to considerably higher frequencies (e.g., to 100 Hz) is dangerous,

Table 2
Non-dimensional eigenfrequency parameters $\Omega = \omega l/c$, $c = (E/\rho)^{1/2}$ of a cable with different inclination angles and lengths, vibrating in vacuum and in water

Inclination angle (θ_c)	Cable length L (m)	Cable model	Out-of-plane (1st)	Out-of-plane (2nd)	In-plane (1st)	In-plane (2nd)
$\pi/6$	987.8	In vacuum	0.0855	0.1708	0.1704	0.2366
		In water	0.0805	0.1609	0.1629	0.2258
			−0.00033i	−0.00066i	−0.00055i	−0.00075i
	1387.8	In vacuum	0.02974	0.05531	0.04548	0.1061
		In water	0.02789	0.05197	.04451	0.1032
			−0.0002i	−0.00031i	−0.00041i	−0.00061i
$\pi/4$	1209.9	In vacuum	0.06972	0.1393	0.1376	0.1932
		In water	0.06555	0.1311	0.1333	0.1869
			−0.00035i	−0.00048i	−0.00066i	−0.00078i
	1609.9	In vacuum	0.02684	0.05084	0.03980	0.0959
		In water	0.02518	0.04775	0.03905	0.08851
			−0.00023i	−0.0003i	−0.00042i	−0.00059i
$\pi/3$	1711.0	In vacuum	0.04960	0.09915	0.09556	0.1372
		In water	0.04657	0.09325	0.09370	0.1344
			−0.00029i	−0.00029i	−0.00064i	−0.00079i
	2111.0	In vacuum	0.02239	0.04363	0.03173	0.06911
		In water	0.02095	0.04098	0.03119	0.06784
			−0.0002i	−0.00038i	−0.00039i	−0.00055i

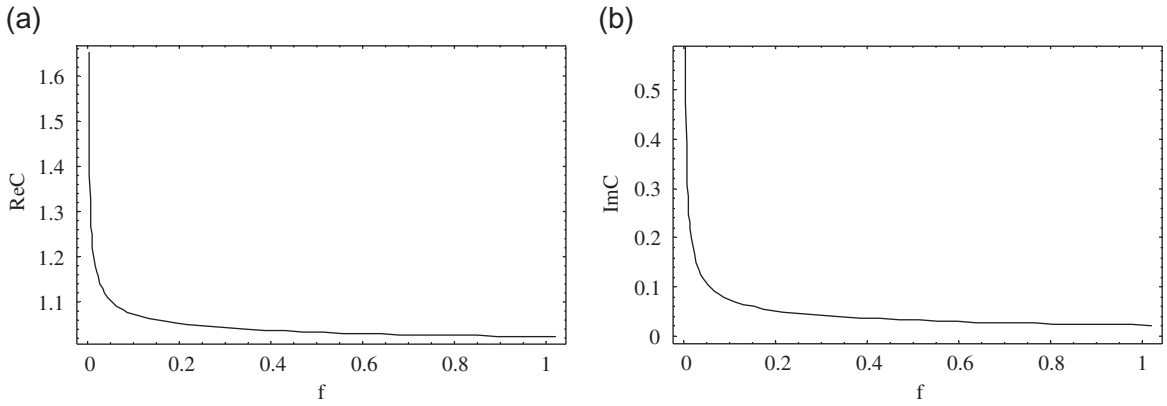

Fig. 7. (a) The added mass coefficient and (b) the damping coefficient versus frequency in Hertz.

because in a relatively high-frequency regime the laminar flow becomes unstable and the damping properties of the fluid become controlled by the turbulent motion. On the other hand, predictions of this asymptotic model for extremely low frequencies (which are not actually of considerable practical interest) are also not adequate because the exact formulation of the coefficients should be used. However, it is remarkable that the regime of linear motion identified in Srinil et al. (2003) for a cable vibrating in vacuum lies exactly within the range of validity of the suggested theory.

4. Numerical examples: added mass and viscous damping effects for cables vibrating in air and in water

To determine eigenfrequencies of a cable submerged in water, time dependence is selected as $\exp(-i\omega t)$ and the motion Eq. (7) are formulated with respect to displacement components, because the hydrodynamic forces are

expressed analytically through Eqs. (24), (25) and (28). They read

$$\frac{Tu''}{\sqrt{1+(y')^2}}+\left[\frac{EA}{\sqrt{1+(y')^2}}(u'+y'v')\right]'+\sqrt{1+(y')^2}\omega^2\rho Au\left(1+\frac{T}{EA}\right)^{-1}+2\pi i\rho_{fl}v_{fl}\omega u\eta_1=0,$$

$$\frac{Tv''}{\sqrt{1+(y')^2}}+\left[\frac{EA}{\sqrt{1+(y')^2}}\left(y'u'+(y')^2v'\right)\right]'+\sqrt{1+(y')^2}\omega^2\rho Av\left(1+\frac{T}{EA}\right)^{-1}+\rho_{fl}\omega^2v\pi R^2\left(1-\frac{4}{\eta}\right)=0,$$

$$\frac{Tw''}{\sqrt{1+(y')^2}}+\sqrt{1+(y')^2}\omega^2\rho Aw\left(1+\frac{T}{EA}\right)^{-1}+\rho_{fl}\omega^2w\pi R^2\left(1-\frac{4}{\eta}\right)=0. \tag{30}$$

Again, the eigenfrequencies are found by use of the Galerkin method and expansions (9). However, the structure of fluid-loading terms in Eqs. (30) is rather complicated, even when asymptotic formulas (29) are applied. It is impossible to obtain the characteristic equation in the elementary polynomial form, as done in Section 2 for a cable vibrating in vacuum. The standard approach to detect eigenfrequencies is to 'sweep' over the frequency range in search for the minima of the frequency determinant. Inasmuch as viscous effects in a fluid are taken into account, this determinant cannot vanish at any purely real frequency. Then the complex-valued eigenfrequency is determined by *Mathematica*, with an initial guess in the numerical procedure being chosen as a purely real frequency at which the module of the characteristic determinant has its minimum. The imaginary part of an eigenfrequency characterises the rate of decay of free vibrations.

Naturally, the static equilibrium configuration of a cable submerged into water $y(x)$ should be found with the buoyancy force taken into account. It is a fairly trivial task accomplished by replacing the actual weight per unit cable length ρg by its effective magnitude $(\rho-\rho_{fl})g$ (reduced by the buoyancy force) in solving the static equilibrium problem. However, in all examples reported hereafter, the static equilibrium configuration of the cable in water is almost exactly the same as in air due to the large density of the considered cable material. Yet, it is observed that this difference could be very much pronounced if a non-metallic (light) cable is considered. This—apparently practically meaningful—case is deliberately left out here, since the subject of the present paper is the role of water in dynamics rather than in statics of a submerged cable. Eqs. (30) involve non-reduced density of cable material ρ.

The eigenfrequency nondimensional parameters $\Omega=\omega l/c$, $c=(E/\rho)^{1/2}$ are computed for the same inclined cables as in Section 2 both in air and in water. In the case of vibrations in air, the contribution of the added mass is negligible and the equivalent viscous damping is of order 10^{-7}. Then the effects of interaction between cable and air at rest are totally negligible. This result is fairly trivial, and indeed the interaction between a vibrating cable and an otherwise quiescent air has never been considered in the literature on cable dynamics. However, it is worth noting that herein this general assessment has been quantified.

The results for vibrations in water are summarised in Tables 2–4. Table 2 presents the non-dimensional complex-valued eigenfrequencies in water and—as a reference—their counterparts for vibrations in air. The usual three inclination angles are considered, and the frequency parameters are listed for the minimum and maximum cable lengths discussed in connection to Table 1.

The modal added mass can be readily assessed using the data presented in Table 2. Indeed, in the linear treatment of the free vibration problem, each modal eigenfrequency ω_m in the absence of damping is formulated via the modal stiffness K_m and the modal mass M_m as $\omega_m^2=K_m/M_m$. Then the modal added mass coefficient appears to be $\delta=(\omega^2_{m,\text{vacuum}}/\omega^2_{m,\text{water}})-1$. Its values are summarised in Table 3. Several important conclusions can be derived from these data. First of all, the modal added mass coefficient is strongly dependent on the frequency and the mode shape. It is remarkable that the values for the out-of-plane vibrations are considerably larger than for the in-plane ones. Moreover, the modal added mass coefficients for the out-of-plane vibrations are larger than the value (determined by the density ratio $\rho_{\text{water}}/\rho\approx0.12$) suggested by the elementary model of interaction between an incompressible inviscid fluid and an infinitely long cylindrical body performing oscillations in the direction perpendicular to its axis. The magnitude of the added mass coefficient for the out-of-plane modes slightly grows as the inclination angle increases. The influence of the fluid on in-plane modes is very different from that on out-of-plane modes. In all reported cases, the added mass coefficient of in-plane modes is substantially less than the above-mentioned 'threshold value' $\rho_{\text{water}}/\rho\approx0.12$ (defined for 'cross-axis' motion of a rigid cylinder). It diminishes as the inclination angle increases and it is slightly smaller for the first mode than for the second one.

Table 3
Modal added mass coefficients of a cable with different inclination angles and lengths, vibrating in water

Inclination angle (θ_c)	Cable length L (m)	Out-of-plane (1st)	Out-of-plane (2nd)	In-plane (1st)	In-plane (2nd)
$\pi/6$	987.8	0.128	0.127	0.094	0.098
	1387.8	0.137	0.133	0.044	0.057
$\pi/4$	1209.9	0.131	0.129	0.066	0.069
	1609.9	0.136	0.134	0.039	0.048
$\pi/3$	1711.0	0.134	0.131	0.040	0.042
	2111.0	0.142	0.134	0.035	0.038

Table 4
Modal damping coefficients of a cable with different inclination angles and lengths, vibrating in water

Inclination angle (θ_c)	Cable length L (m)	Out-of-plane (1st)	Out-of-plane (2nd)	In-plane (1st)	In-plane (2nd)
$\pi/6$	987.8	0.00410	0.00410	0.00338	0.00332
	1387.8	0.00717	0.00596	0.00921	0.00591
$\pi/4$	1209.9	0.00534	0.00366	0.00495	0.00417
	1609.9	0.00913	0.00628	0.0108	0.00667
$\pi/3$	1711.0	0.00623	0.00440	0.00683	0.00588
	2111.0	0.00955	0.00927	0.0125	0.00811

The overall difference of the added mass coefficients between out-of-plane and in-plane mode has an elementary physical explanation. As stated in the previous section, the viscous effects manifest themselves differently in the 'cross-axis' motions of a cable and in its 'sliding' motions. Specifically, in a case of 'cross-axis' motions viscous fluid contributes both the added mass and the viscous damping, and the former effect can be predicted by use of the model of inviscid fluid. In a case of 'sliding' motions of a cable, the fluid also produces both these effects, but only due to its viscosity. Indeed, there is no interaction between the structure and an inviscid fluid at all in the case of 'sliding' motion. The out-of-plane vibrations of a cable are dominantly lateral (i.e., the principal direction of motion is perpendicular to the cable axis), whereas the in-plane vibrations involve quite substantial longitudinal components of displacement, as apparent from Figs. 4 and 6. Therefore, the resulting inertial effect is set up as a combination of these two components. As the 'sliding' longitudinal component practically affects only the in-plane vibrations, the added mass is smaller than in out-of-plane vibrations due to the effect of fluid viscosity. As is seen from Table 3, the added mass coefficient remains approximately the same for the first and the second mode in each case for each type of motion.

The ratio of the imaginary part of an eigenfrequency to its real part gives a value of equivalent viscous damping coefficient (Rao, 2004) for each mode (note that the logarithmic decrement is 2π times larger). These data are summarised in Table 4. As is seen, the modal equivalent damping is rather large and its magnitude is 'modal dependent'. The general trend observed in all considered cases is obvious: the damping coefficient increases as the cable becomes longer. This is explained simply by the increase of the friction force resultant of the stresses distributed along the cable due to the increase in the 'wetted' surface area. The difference in magnitudes of modal damping coefficients between in-plane and out-of-plane modes has a similar explanation as the difference in added mass coefficients: the axial components of displacement characterising the in-plane modes have a major contribution in long cables (as suggested by the analysis of the mode shapes), and this entails greater values of the relevant in-plane damping coefficients than the out-of-plane ones.

From the reported results, it should be concluded that both the added mass coefficient and the damping coefficient vary in a relatively broad range for a cable of given parameters, depending on its length and the mode under consideration. Thus, it is very questionable to use the elementary added mass coefficient ρ_{water}/ρ and to ignore the energy dissipation effects in water in the case of linear cable vibrations. On the other hand, the role of acoustic emission in the given excitation conditions is totally negligible. All calculations have been carried out for a metallic cable. Apparently, the density ratio ρ_{water}/ρ for non-metallic cables is substantially larger and, therefore, the added mass effect should be much stronger.

5. Summary and suggestions for further research

The main results reported in this paper are summarised as follows:

(i) a theory to describe the linear time-harmonic behaviour of an arbitrarily sagged inclined cable under heavy fluid loading by a viscous fluid has been presented;
(ii) the ensuing evaluated added mass and viscous damping coefficients have been shown to be strongly dependent on the type of mode, and this dependence has been explained.

This entails that considering too simple (e.g., constant) approximations of the added mass value which do not account for the water damping and frequency-dependent inertia features may be quite unreliable.

Moreover, within a previous analysis of arbitrarily sagged inclined cables in air—aimed at identifying the proper equilibrium shape to be referred to in the investigation of fluid-cable dynamic interaction—it has been computationally documented that the inextensible catenary equilibrium shape (usefully available in closed form) may be reliably used in all cases, when the cable has a sufficiently large sag-to-span ratio. However, while there is virtually no difference between incorporating into the analysis a cubic approximation or the "exact" catenary shape, the numerical accuracy of the former becomes unsatisfactory when the lowest cable point does not coincide with one of its supports.

Further research into vibrations of cables submerged into water should encompass the analysis of weakly nonlinear effects. Different sources of nonlinearity should affect the formulation of such a problem. A first group is concerned with the structural behaviour, and is represented by the quadratic and cubic nonlinearities occurring in the expansion of Eq. (5) as a result of moderately large cable vibration amplitudes, but it could also involve the nonlinear constitutive equation to be considered for a cable made of PVC or other nonideally elastic materials. The second and the third sources of nonlinearity are instead associated with the behaviour of the fluid described by Navier–Stokes equations and with the formulation of continuity conditions for velocities of the structure and the fluid at the moving fluid–structure interface, respectively. To this end, it might be unrealistic to aim at a 'full scale' modelling of the fluid motion, which involves transition to a turbulent regime, etc., in further analysis. Possibly, a reasonably good estimate of the influence of 'fluid-induced' nonlinearity could be obtained by still considering linear Navier–Stokes equations, but with the continuity conditions involving nonlinear terms. It should be pointed out that such an approach has already been validated for problems in nonlinear vibrations of elastic structures under heavy fluid loading (Sorokin and Kadyrov, 1999; Sorokin and Chapman, 2005). Another observation supports the meaningfulness of a weakly nonlinear approach to fluid–cable dynamics: it is not realistic to expect all of the effects of strong galloping and ballooning, which characterise the dynamics of cables in air (Rega, 2004b), to be developed to the same extent in the case of a cable submerged into water.

References

Chang, W.K., Pilipchuk, V., Ibrahim, R.A., 1997. Fluid flow-induced nonlinear vibration of suspended cables. Nonlinear Dynamics 14, 377–406.

Der Kiureghian, A., Sackman, J.L., 2005. Tangent geometric stiffness of inclined cables under self-weight. Journal of Structural Engineering, 941–945.

Guz, A.N., 1981. Dynamics of solid bodies in a compressible viscous quiescent fluid. Prikladnaya Mekhanika 18 (3), 3–22 (in Russian).

Hu, H.Y., Jin, D.P., 2001. Nonlinear dynamics of a suspended traveling cable subject to transverse fluid excitation. Journal of Sound and Vibration 239, 515–529.

Ibrahim, R.A., 2004. Nonlinear vibrations of suspended cables—Part III: random excitation and interaction with fluid flow. Applied Mechanics Reviews 57 (6), 515–549.

Irvine, H.M., 1981. Cable Structures. MIT Press, Cambridge, MA.

Irvine, H.M., Caughey, T.K., 1974. The linear theory of free vibrations of a suspended cable. Proceedings of the Royal Society of London A 341, 299–315.

Junger, M.G., Feit, D., 1993. Sound, Structures and Their Interaction, second ed. MIT Press, Cambridge, MA.

Kadyrov, S.G., Wauer, J., Sorokin, S.V., 2001. A potential technique in the theory of interaction between a structure and a viscous, compressible fluid. Archive of Applied Mechanics 71, 405–417.

Landau, L.D., Livshitz, E.M., 1987. Fluid Mechanics, second ed. Pergamon, Oxford.

Merkin, D.R., 1980. Introduction to Mechanics of a Flexible Thread. Nauka, Moscow (in Russian).

Milne-Thompson, L.M., 1988. Theoretical Hydrodynamics, fifth ed. Dover, New York.

Morison, D., O'Brien, M., Johnson, J., Schaaf, S., 1950. The force exerted by surface waves on piles. Petroleum Transactions American Institute of Mining Engineers 189, 149–154.

Rao, S.S., 2004. Mechanical Vibrations, fourth ed. Pearson, Prentice-Hall, Englewood Cliffs, NJ.

Rega, G., 2004a. Nonlinear vibrations of suspended cables—Part I: modeling and analysis. Applied Mechanics Reviews 57 (6), 443–478.

Rega, G., 2004b. Nonlinear vibrations of suspended cables—Part II: deterministic phenomena. Applied Mechanics Reviews 57 (6), 479–514.

Russell, J.C., Lardner, T.J., 1998. Experimental determination of frequencies and tension for elastic cables. American Society of Civil Engineers Journal of Engineering Mechanics 124, 1067–1072.

Sorokin, S.V., Chapman, C.J., 2005. Asymptotic analysis of vibration of an elastic plate under heavy fluid loading. Journal of Sound and Vibration 284, 1131–1144.

Sorokin, S.V., Kadyrov, S.G., 1999. Modelling of nonlinear oscillations of elastic structures in heavy fluid loading conditions. Journal of Sound and Vibration 222, 425–451.

Srinil, N., Rega, G., Chucheepsakul, S., 2003. Large amplitude three-dimensional free vibrations of inclined sagged elastic cables. Nonlinear Dynamics 33, 129–154.

Srinil, N., Rega, G., Chucheepsakul, S., 2004. Three-dimensional nonlinear coupling and dynamic tension in the large-amplitude free vibrations of arbitrary sagged cables. Journal of Sound and Vibration 269, 823–852.

Srinil, N., Rega, G., Chucheepsakul, S., 2007. Two-to-one resonant multi-modal dynamics of horizontal/inclined cables. Part I: theoretical formulation and model validation. Nonlinear Dynamics 48, 231–252.

Triantafyllou, M.S., Grinfogel, L., 1986. Natural frequencies and modes of inclined cables. Journal of Structural Engineering 112, 421–440.

Wolfram, S., 1991. Mathematica: a system for doing mathematics by computer. Addison-Wesley Publishing Co., Reading, MA.

Wu, Q., Takahashi, K., Nakamura, S., 2005. Formulae for frequencies and modes of in-plane vibrations of small-sag inclined cables. Journal of Sound and Vibration 279, 1155–1169.

Zheng, G., Ko, G.M., Ni, Y.Q., 2002. Super-harmonic and internal resonances of a suspended cable with nearly commensurable natural frequencies. Nonlinear Dynamics 30, 55–70.